

# CHARACTERIZING 1-YEAR DEVELOPMENT OF CERVICAL CORD ATROPHY ACROSS DIFFERENT MS PHENOTYPES: A VOXEL-WISE, MULTICENTER ANALYSIS

<sup>1</sup>Paola Valsasina, <sup>6</sup>Claudio Gobbi, <sup>6</sup>Chiara Zecca, <sup>7</sup>Alex Rovira, <sup>8</sup>Jaume Sastre-Garriga, <sup>9,10</sup>Hugh Kearney, <sup>10</sup>Marios Yiannakas, <sup>11</sup>Lucy Matthews, <sup>11</sup>Jacqueline Palace, <sup>12</sup>Antonio Gallo, <sup>12</sup>Alvino Biseco, <sup>13</sup>Achim Gass, <sup>13</sup>Philipp Eisele, <sup>1,2,3,4,5</sup>Massimo Filippi, <sup>1,2,5</sup>Maria A. Rocca, for the MAGNIMS Study Group\*.

<sup>1</sup>Neuroimaging Research Unit, Division of Neuroscience, <sup>2</sup>Neurology Unit, <sup>3</sup>Neurorehabilitation Unit and <sup>4</sup>Neurophysiology Service, IRCCS San Raffaele Scientific Institute, Milan, Italy; <sup>5</sup>Vita-Salute San Raffaele University, Milan, Italy; <sup>6</sup>Multiple Sclerosis Center, Department of Neurology, Neurocenter of Southern Switzerland, Civic Hospital, Lugano, Switzerland; Faculty of Biomedical Sciences, Università della Svizzera Italiana (USI); <sup>7</sup>Section of Neuroradiology, Department of Radiology, Hospital Universitari Vall d'Hebron, Barcelona, Spain; <sup>8</sup>Department of Neurology/Neuroimmunology, Multiple Sclerosis Center of Catalonia, Hospital Universitari Vall d'Hebron, Barcelona, Spain; <sup>9</sup>Department of Neurology, St Vincent's University Hospital, Dublin, Ireland; <sup>10</sup>NMR Research Unit, Queen Square MS Centre, Department of Neuroinflammation, UCL Institute of Neurology, London, UK; <sup>11</sup>Nuffield Department of Clinical Neurosciences, University of Oxford, Oxford, UK; <sup>12</sup>Department of Advanced Medical and Surgical Sciences and 3T-MRI Research Centre, University of Campania "Luigi Vanvitelli", Naples, Italy; <sup>13</sup>Department of Neurology/Neuroimaging, Medical Faculty Mannheim and Mannheim Center for Translational Neurosciences (MCTN), University of Heidelberg, Mannheim, Germany;

\***MAGNIMS Study group:** <sup>14,15</sup>Frederik Barkhof, <sup>9</sup>Olga Ciccarelli, <sup>16</sup>Nicola De Stefano, <sup>17</sup>Christian Enzinger, <sup>1,2,3,4,5</sup>Massimo Filippi, <sup>18</sup>Claudio Gasperini, <sup>19</sup>Ludwig Kappos, <sup>11</sup>Jacqueline Palace, <sup>1,2,5</sup>Maria A. Rocca, <sup>7</sup>Alex Rovira, <sup>8</sup>Jaume Sastre-Garriga, <sup>14</sup>Hugo Vrenken, <sup>9</sup>Tarek Yousry

<sup>14</sup>Department of Radiology and Nuclear Medicine, MS Center Amsterdam, VU University Medical Center, Amsterdam, The Netherlands; <sup>15</sup>Institutes of Neurology and Healthcare Engineering, University College London, UK; <sup>16</sup>Department of Medicine, Surgery and Neuroscience, University of Siena, Siena, Italy; <sup>17</sup>Department of Neurology, Medical University of Graz, Graz, Austria; <sup>18</sup>Department of Neurosciences, San Camillo-Forlanini Hospital, Rome, Italy; <sup>19</sup>Research Center Clinical Neuroimmunology and Neuroscience Basel (RC2NB), Departments of Medicine, Clinical Research, and Biomedicine and Biomedical Engineering, University Hospital and University of Basel, Basel, Switzerland.

**Article type:** Original Research

**Text word count:** 3359. **Abstract:** 200. **Number of tables:** 3. **Number of figures:** 5.

**Supplementary files:** Supplementary Tables 1-3; Supplementary Figure 1. **Number of references:** 35.

**Study funding:** The project in London was funded by the UK MS Society and supported by the National Institute for Health Research (NIHR) University College London Hospitals (UCLH) Biomedical Research Centre (BRC). This work in Oxford was funded by an MRC fellowship to Dr Lucy Matthews (G0901996).

**Correspondence should be addressed to:** Prof. Maria A. Rocca, Neuroimaging Research Unit, Division of Neuroscience, IRCCS San Raffaele Scientific Institute, Milan, Italy. Telephone number: +39-02-26433019; Fax number: +39-02-26433031; E-mail address: [rocca.mara@hsr.it](mailto:rocca.mara@hsr.it)

## Abstract

**Background.** Spatio-temporal evolution of cord atrophy in MS has not been investigated yet.

**Objective.** To evaluate voxel-wise distribution and 1-year changes of cervical cord atrophy in a multicenter MS cohort.

**Methods.** Baseline and 1-year 3D T1-weighted cervical cord scans and clinical evaluations of 54 healthy controls (HC) and 113 MS patients (14 clinically isolated syndromes [CIS], 77 relapsing-remitting [RR], 22 progressive [P]MS) were used to investigate voxel-wise cord volume loss in patients vs HC, 1-year volume changes and clinical correlations (SPM12).

**Results.** MS patients exhibited baseline cord atrophy vs HC at anterior and posterior/lateral C1/C2 and C4-C6 ( $p < 0.05$ , corrected). While CIS patients showed baseline volume increase at C4 vs HC ( $p < 0.001$ , uncorrected), RRMS exhibited posterior/lateral C1/C2 atrophy vs CIS, and PMS showed widespread cord atrophy vs RRMS ( $p < 0.05$ , corrected). At 1-year, 13 patients had clinically worsened. Cord atrophy progressed in MS, driven by RRMS, at posterior/lateral C2 and C3-C6 ( $p < 0.05$ , corrected). CIS patients showed no volume changes, while PMS showed circumscribed atrophy progression. Baseline cord atrophy at posterior/lateral C1/C2 and C3-C6 correlated with concomitant and 1-year disability ( $r = -0.40/-0.62$ ,  $p < 0.05$ , corrected).

**Conclusions.** Voxel-wise analysis characterized spinal cord neurodegeneration over 1-year across MS phenotypes and helped to explain baseline and 1-year disability.

## Introduction

The spinal cord is clinically eloquent and is often affected by multiple sclerosis (MS).<sup>1</sup> Focal and diffuse lesions, especially in the cervical cord, are common in MS patients,<sup>2</sup> who usually develop cervical cord atrophy, as a result of demyelination and axonal loss.<sup>1</sup>

Cord atrophy occurs in relapsing-remitting (RR) MS, but becomes more severe and prominent in progressive (P) MS phenotypes.<sup>1, 3, 4</sup> Longitudinal assessments found a decrease of cord cross-sectional area (CSA) both in RRMS and in PMS, with variable rates of CSA reduction.<sup>4-7</sup> On the other hand, in patients with clinically isolated syndrome (CIS) cord atrophy seems to be absent or very limited.<sup>4, 8</sup> Cord atrophy is clinically relevant, as confirmed by several studies detecting a significant relationship between CSA reduction and severity of clinical disability.<sup>1, 3-5, 7, 9, 10</sup> Cord atrophy progression may contribute to explain disability worsening at short- or medium-term follow-up (1-5 years),<sup>4, 5, 7</sup> whereas such a relation seems to be lost in longer follow-ups, suggesting a plateauing effect.<sup>11, 12</sup>

Recent advances in image post-processing have allowed a rapid segmentation of the spinal cord along large portions, using a method based on active surfaces (AS)<sup>13</sup> or on deep learning<sup>14</sup> as implemented in the Spinal Cord Toolbox,<sup>15</sup> and the assessment of cord atrophy profiles at different levels. The same method also allowed reformatting the spinal cord perpendicularly to its cord centre line<sup>13, 16</sup> and performing voxel-wise analyses of cervical cord atrophy.<sup>9, 10</sup> This methodology was also used to assess the regional distribution of T2-hyperintense<sup>9, 17</sup> and T1-hypointense<sup>10</sup> cervical cord lesions. To date, these methods have been applied only in cross-sectional studies.

Here, we hypothesized that the application of voxel-wise techniques to longitudinal, high-resolution MRI scans of MS patients may help to characterize the spatial evolution of cervical cord atrophy in disease phenotypes not only at different levels, but also within the transverse cord section. Such a framework may help to identify specific baseline atrophy profiles that may be relevant for concomitant and subsequent disability.

To test this hypothesis, we used voxel-wise analysis to further explore within- and across-plane distribution and changes over 1-year of cervical cord atrophy in a multicenter MS cohort, in which we already characterized global and level-specific cervical cord atrophy in MS.<sup>4</sup> Associations between cord atrophy and baseline and 1-year disability were also investigated.

## **Methods**

Ethics committee approval. Approval was received from Local Ethical standards committees; written informed consent was obtained from all participants prior to enrolment.

Participants. Participants are part (34%) of a prospective cohort ([www.magnims.eu](http://www.magnims.eu)), enrolled between May 2010 and March 2016 in a previous study.<sup>4</sup> All participants underwent a clinical and MRI evaluation at baseline and after 1 year. From the original cohort,<sup>4</sup> we excluded subjects from two centres, because follow-up scans for both healthy controls (HC) and MS patients (necessary for the present analysis) were not available (Figure 1). To be included, MS patients had to have stable treatment during the past 6 months and received no corticosteroids during the last month. CIS patients had to have a first episode suggestive of CNS demyelination and a clinical assessment within three months from clinical symptoms. Exclusion criteria were: history of cervical cord/brain trauma, severe cord compression (radiologically defined) on previous MRI, diagnosis of neuromyelitis optica and other MS mimickers; major comorbidities; history of drug/alcohol abuse; inability to undergo MRI; pregnancy or breastfeeding.

Clinical assessment. Within two days from baseline and 1-year MRI, MS patients underwent a complete neurological evaluation, with rating of the Expanded Disability Status Scale (EDSS) score and functional system (FS) subscores.<sup>18</sup> At 1-year, patients were clinically worsened if EDSS score increased  $\geq 1.0$  point when baseline EDSS was  $< 6.0$ , or if EDSS score increased  $\geq 0.5$  point when baseline EDSS was  $\geq 6.0$ .<sup>19</sup> EDSS changes were confirmed during a second visit after three-months. Disease-modifying treatments and occurrence of relapses during the follow-up were recorded. Considering the similarity of clinical, histopathological and imaging features in primary

and secondary PMS<sup>20</sup> and considering the low number of patients, secondary and primary PMS were grouped together.

MRI acquisition and conventional MRI analysis. All centres used the same 3.0 T scanners at baseline and follow-up (Hospital Vall d'Hebron, Barcelona: Siemens Magnetom Trio; UCL London and IRCCS San Raffaele Scientific Institute: Philips Achieva; Neurocenter of Southern Switzerland, Lugano, and University of Heidelberg, Mannheim: Siemens Magnetom Skyra; University of Campania "L. Vanvitelli", Naples: General Electric Signa HDtx; University of Oxford: Siemens Magnetom Prisma) to acquire sagittal 3D T1-weighted scans covering the whole-cervical cord,<sup>4</sup> used for atrophy analysis. The MRI protocol also included: a) cervical cord sagittal short-tau inversion recovery or T2-weighted/dual-echo fast spin-echo (for cervical cord lesion count); b) brain dual-echo fast spin-echo or T2-fluid-attenuated inversion recovery (for brain T2-hyperintense lesion volume (LV) assessment); and c) brain sagittal 3D T1-weighted (for T1-hypointense LV and global brain volumetry assessment) (Supplementary Table 1).<sup>4</sup>

Cord atrophy assessment. Figure 2 shows the main workflow of MRI data processing. Sagittal T1-weighted cervical cord images underwent axial reformatting and 1-mm thickness resampling to obtain normalized cord CSA between C1 and C7 with the AS method and the Jim software.<sup>4, 13</sup> Baseline and follow-up cord images and binary cord masks were straightened in planes perpendicular to the estimated cord centre line.<sup>13</sup> This was necessary to reduce differences in cord curvature between time points, due to variability of subject's positioning within the scanner, and to allow subsequent image registration.<sup>6, 21</sup> Then, baseline and 1-year T1-weighted cord images from all HC were non-linearly registered using SPM12 and pairwise registration,<sup>22</sup> generating an unbiased half-way cord image for each subject. Interparticipant neck length variability was corrected by rescaling images to the median cervical cord length of HC (i.e, 117 mm); inter-center geometry differences were adjusted by cropping all images to the common inner field-of-view (66x246 mm<sup>2</sup>). Straightened T1-weighted cord images and corresponding masks from HC and MS patients were then rigidly co-registered (using trilinear interpolation to save cord output masks) to

average half-way HC cord image from all sites, serving as cord template, using Jim7. Specifically, rigid registration consisted of a translation and rotation in the x-y plane and a scaling factor along the cranio-caudal direction.<sup>10, 16</sup> This was done to avoid deforming cord masks and to minimize any bias on subsequent atrophy evaluation. Finally, cord masks were smoothed (full-width at half maximum Gaussian kernel=1x1x2 mm<sup>3</sup>).<sup>16</sup>

Statistical analysis. Brain T2 LV and T1 LV were log transformed. Baseline comparisons of demographic, clinical and conventional brain and cord MRI measures between HC and MS patients and among phenotypes were performed using two-sample t tests, Chi-square tests (as appropriate according to data normality), Kruskal-Wallis tests and ANOVA models adjusted for age, sex and site (SPSS software, version 26.0). The following *post hoc* contrasts were used: HC vs CIS, CIS vs RRMS, and RRMS vs PMS. Repeated-measures ANOVA models adjusted for age, sex, site and follow-up duration assessed longitudinal changes of clinical/conventional MRI metrics, using the above-mentioned *post hoc* contrasts.

The voxel-wise analysis of cord atrophy distribution was performed using SPM12, including age, sex and site (and follow-up duration for longitudinal analyses) as confounding covariates. Total cord volume was also included as confounding covariate to privilege the detection of regional on whole-cord atrophy differences. Full factorial models assessed baseline and 1-year cord atrophy differences between HC and MS patients and among phenotypes. Within-group voxel-wise changes of cord atrophy over time were investigated using paired t tests, while time-by-group interactions of cord atrophy progression were tested using full factorial models.

Linear regression models (SPSS 26.0) assessed correlations between: 1) baseline clinical and baseline cord/brain MRI metrics; and 2) follow-up EDSS score and baseline cord/brain MRI metrics (including also baseline EDSS as confounding covariate). Likewise, SPM12 multiple regression models assessed correlations of baseline regional cord atrophy with: 1) baseline clinical/conventional MRI variables; and 2) follow-up EDSS score (including also baseline EDSS as confounding covariate). Results were tested at  $p < 0.05$ , clusterwise family-wise error (FWE)

corrected for multiple comparisons; uncorrected results ( $p < 0.001$ ) were also reported. Clusters of cord atrophy surviving at these two statistical thresholds were then superimposed on a custom-made region-label cord mask in the normalized space to label atrophy clusters.<sup>10, 16</sup>

Validation analysis. To test stability of our results against the multicenter study design, we repeated the main regional cord atrophy statistical analyses using subjects from one site only (IRCCS San Raffaele Scientific Institute).

## Results

Demographic, clinical and conventional MRI. Sixty-three HC and 148 MS patients were screened. After excluding 9 HC and 35 MS patients because of inadequate image post-processing (artefacts,  $n=4$  HC/10 MS; unsuccessful registration,  $n=5$  HC/15 MS, Figure 1), data from 54 HC and 113 MS patients were finally included. There were 14 CIS, 77 RRMS and 22 PMS patients (Table 1), with the following distribution:  $n=5/13$  HC/MS from Barcelona;  $n=7/15$  HC/MS from London;  $n=9/29$  HC/MS from Lugano;  $n=5/12$  HC/MS from Mannheim;  $n=14/22$  HC/MS from Milan;  $n=6/14$  HC/MS from Naples; and  $n=8/8$  HC/MS from Oxford. MS patients were not significantly different from HC in terms of global brain volume and whole-cervical CSA (Table 1). EDSS score, disease duration and treatment were heterogeneous among MS phenotypes. Brain T2 LV ( $p < 0.001$ ) and T1 LV ( $p = 0.001$ ) were higher in RRMS vs CIS, but not different between RRMS and PMS patients. There was a trend ( $p = 0.1$ ) towards a lower normalized CSA in RRMS vs CIS, becoming significant ( $p < 0.001$ ) in PMS vs RRMS patients. Cord lesion number did not differ across phenotypes (Table 1).

The median follow-up duration was 1.01 years (interquartile range=0.98-1.15 years) in HC and 1.09 years (interquartile range=0.99-1.27 years) in MS patients ( $p = 0.14$ ). Four patients evolved from CIS to RRMS; 4 evolved from RRMS to PMS. EDSS score did not change over time in the whole MS group ( $p = 0.25$ ). Thirteen patients (12%) had clinically worsened at 1-year.

Brain T2 LV ( $p=0.1$ ) and T1 LV ( $p=0.9$ ) were stable over time. Whole-cord atrophy progression was significantly higher in MS patients vs HC (Table 1), but not different in RRMS vs CIS ( $p=0.2$ ), nor in RRMS vs PMS patients ( $p=0.6$ ). The median number of new cord lesions at follow-up was 0 and the percentage brain volume change was not significantly different among groups (Table 1).

Voxel-wise cervical cord atrophy analysis. *Findings at baseline.* Cord atrophy in MS patients vs HC was localized in the anterior, posterior and lateral cord columns at C1/C2, and in the lateral and posterior cord between C3 and C6 ( $p<0.05$ , FWE, Figure 3, Table 2).

When looking at clinical phenotypes, we found volume increase in CIS patients vs HC in the posterior/lateral cord at C4 ( $p<0.001$ , uncorrected) (Figure 3, Table 2), while RRMS had significant atrophy vs CIS mainly in the posterior and lateral cord columns at C1/C2 ( $p<0.05$ , FWE), and PMS showed widespread cord atrophy vs RRMS patients ( $p<0.05$ , FWE), especially posteriorly/laterally at C3, C4, C5, C6 and C7 (Figure 3, Table 2).

*Findings at follow-up.* Cord volume remained stable in HC during the follow-up. In MS patients, cervical atrophy progressed in the posterior and lateral cord columns at C1/C2, and between C4 and C6 ( $p<0.05$ , FWE) (Figure 4, Table 3) and was significantly greater at C1/C2 than in HC at time-by-group interaction analysis ( $p<0.001$ ).

Such pattern was mainly driven by RRMS, who showed a pronounced cord atrophy progression in these regions ( $p<0.05$ , FWE). Cord volume did not change significantly in CIS, who exhibited cord volume increase vs HC ( $p<0.001$ , uncorrected) in the posterior/lateral cord at C4 at 1-year. Cord atrophy developed in the posterior/lateral cord at C1/C2, C3 and C5 in PMS patients ( $p<0.001$ , uncorrected) (Figure 4, Table 3). Results did not change when including baseline treatment/treatment change as additional confounding covariates (data not shown). Also, results obtained using single-site data resembled those obtained using the whole study cohort, as shown in Supplementary Tables 2 and 3, and Supplementary Figure 1.

Correlation analysis. In MS patients, a higher baseline EDSS and a longer disease duration were associated with higher brain T2 LV, T1 LV and cord lesion number (beta=range 0.19 to 0.28, p=range 0.01 to 0.001). No correlations were found between clinical variables vs whole-brain volumes and whole-cord CSA, both at baseline and follow-up.

At voxel-wise analysis, significant associations were found between baseline cervical cord atrophy, especially in lateral C1/C2 and between C3 and C6, and baseline EDSS score (r=range -0.40 to -0.62,  $p < 0.05$  FWE, Figure 5). This association was mainly driven by the pyramidal FS (r=range -0.46 to -0.59,  $p < 0.05$  FWE) and sphincteric FS (r=-0.55,  $p < 0.05$  FWE) (Figure 5), while the remaining FS subscores were not correlated with cervical cord atrophy. In addition, baseline cord tissue loss in lateral regions between C3 and C6 was associated with a longer disease duration (r=range -0.45 to -0.59,  $p < 0.05$  FWE). Higher T2 and T1 LV (r=range -0.37 to -0.41,  $p < 0.05$  FWE) and lower whole-brain volume (r=range 0.40 to 0.49,  $p < 0.001$  uncorrected) were associated with cord atrophy at posterior C6 and anterior C1/C2. Finally, a higher follow-up EDSS score was predicted by higher baseline cervical cord atrophy in posterior/anterior C4-C6 regions (r=range -0.77 to -0.87,  $p < 0.05$  FWE, Figure 5).

## **Discussion**

In this study, a voxel-wise, longitudinal technique allowed us to obtain a detailed characterization of the spatio-temporal distribution of cord atrophy in a relatively large, multicenter MS group and to investigate correlations with clinical disability at baseline and after 1-year of follow-up.

Considering baseline cord/brain atrophy assessment, whole-cervical cord normalized CSA and normalized brain volume were not significantly lower in MS patients than HC, a finding probably related to the high proportion of CIS and RRMS. Despite this, a regional loss of cord tissue, significant at corrected threshold, was detected. In line with previous voxel-wise MRI studies<sup>9, 10, 16</sup> and pathological data,<sup>23</sup> atrophy clusters were mainly located along the posterior and

lateral cord boundaries. This suggests a higher sensitivity of regional than global atrophy quantification, with global assessment probably being able to disclose a significant cord involvement when diffuse cord tissue loss exceeds a certain extent. In addition, results indicate a greater vulnerability to MS-related damage of posterior and lateral rather than anterior cord columns, resembling previous lesional,<sup>10</sup> atrophy<sup>4, 10</sup> quantitative MRI<sup>24-27</sup> and pathological<sup>23</sup> investigations.

Baseline cord atrophy location in the different MS phenotypes also presented some interesting features. While CIS patients showed circumscribed cord volume increase in the posterior/lateral cord at C3/C4, cervical cord tissue loss was significant in RRMS in the lateral cord at C1/C2, and was more severe and widespread at all cord levels in PMS patients. Previous studies generally detected no cord atrophy in CIS patients *vs* HC;<sup>4, 8, 9</sup> however, some evidence of increased cord volume at early disease stages was found,<sup>28</sup> which might be due to inflammation or edema-related expansion. In line with previous studies,<sup>4, 9, 10</sup> cord atrophy in RRMS patients was limited to the lateral columns at C1/C2. Conversely, in PMS patients atrophy was distributed across all levels, reinforcing the notion that severe cord tissue loss is a typical feature of progressive phases<sup>1, 16</sup> and that a cranio-caudal gradient of cord involvement occurs over MS disease course.<sup>4</sup>

The novel analysis method we used allowed to define the spatial profiles of cord atrophy progression across and within cord levels, which were never investigated before. To date, voxel-wise studies of cord volume loss were performed only cross-sectionally.<sup>9, 10, 16</sup> The extension to longitudinal designs required registering straightened baseline and follow-up cord T1-weighted images in a half-way space, used for the creation of a reference cord template. This was achieved by using symmetric diffeomorphic registration,<sup>22</sup> which was originally tested on brain 3D T1-weighted images, but was potentially designed to work with any pair of longitudinal MRI scans, also acquired from other structures than the brain.<sup>22</sup> As illustrated in Figure 2, the workflow of data processing required several steps, each potentially introducing some uncertainty. The most critical steps were indeed the pair-wise and the rigid registration, failing in 20 subjects. Nevertheless, such analysis

was feasible in the majority of study subjects, and was sensitive enough to detect gradients of cord atrophy progression in line with MS pathophysiology. The application of this technique to other conditions characterized by an uneven distribution of cord damage (e.g., amyotrophic lateral sclerosis, infectious diseases, vitamin B12 deficiency) might be appealing to monitor cord damage progression and potential effects of treatment.

Our analysis confirmed a significant reduction of cord volume over time in all phenotypes, except for CIS, whose cord appear to be ‘swollen’ when compared to HC even after 1-year. This reinforces the notion that cord atrophy progression is a hallmark of established MS,<sup>4-6, 29</sup> while cord inflammation seems to be prevalent in CIS patients.<sup>4, 8, 30</sup> Stability of cord volume over time may also be explained by the low proportion of CIS (n=3, 23%) converting to RRMS during the follow-up, and by the lack of use of disease-modifying treatments in this group. Interestingly, atrophy progression occurred in the remaining MS phenotypes even if the number of new cervical cord lesions at 1-year was very low, suggesting a relative independence between new lesion formation and cord volume loss. The most hit cord regions were posterior regions at C1/C2 and C4 (significant at the time-by-group interaction analysis *vs* HC). Once again, these data confirm that the upper cervical cord is particularly vulnerable to MS,<sup>4, 10, 31</sup> possibly because of a higher myelin content and white matter fiber density. Also, the preferential involvement of the posterior cord suggests a greater susceptibility to MS-related damage of dorsal columns.<sup>24, 26, 32</sup> Contrary to some previous studies<sup>5, 7</sup> but in line with others,<sup>4, 33</sup> we did not find a clear-cut difference of atrophy progression rates between RRMS and PMS. However, RRMS patients exhibited the most widespread pattern of cord tissue loss at 1-year *vs* baseline. This may be due to early inflammation to be resolved, more evident progression of demyelination and axonal loss in this phenotype compared to PMS, or the presence of gliosis and reactive astrocytosis in this latter group.<sup>4, 34, 35</sup> On the other hand, the limited sample size of PMS patients may have also played a role.

Baseline cervical cord atrophy, especially in posterior regions between C4 and C6, was associated with clinical disability and disease duration. Of note, there was a peculiar correlation

between cord atrophy and pyramidal and sphincteric FS, reinforcing the importance of cord damage to explain locomotor impairment<sup>16</sup> and bladder or bowel control problems. Moreover, cord atrophy and brain damage were associated (in terms of lesion extent and brain volume loss), suggesting that cord tissue loss might be, at least partially, originated by Wallerian degeneration of long-fiber tracts.

Baseline cord atrophy in the posterior and anterior cord at C4/C5 had a significant association with clinical disability at 1-year follow-up (adjusted for baseline disability). This is not the first study showing an association between cord atrophy and short-term disease progression,<sup>4, 5, 7</sup> and reinforces the importance of cord damage in explaining subsequent disease course, at least when follow-up duration is relatively short.

This study is not without limitations. First, we had to discard images from a relatively large number of subjects, since the current analysis technique is sensitive to even small quality issues. This may limit the applicability to a clinical setting. Second, the PMS group was relatively small, thus hampering a separate investigation of secondary and primary PMS patients. Third, age was different among study groups; however, it was included as confounding covariate in all statistical models. Fourth, the follow-up duration was quite short; as a consequence, the number of clinically worsened MS patients (n=13) was too small for a separate analysis. Fifth, due to inadequate image quality for cord tissue segmentation, atrophy was quantified on binary cord masks. Sixth, we used a post-processing based on cord volumes; future studies may implement analysis pipelines able to work directly on active shapes. Finally, rate of atrophy development over time might be close to the intrinsic method precision; future studies may better elucidate how reliable are regional atrophy results over longer follow-up periods.

To conclude, cord atrophy progressed differentially across and within cervical cord levels according to MS phenotypes. Baseline cord atrophy correlated with concomitant motor disability and predicted clinical impairment at 1-year. Given the ability of this technique to highlight the differential cord involvement across phenotypes, and to disclose cord regions most hit by MS

pathology, such an approach might be useful to support future pharmacological and rehabilitative decisions for MS patients.

## **Conflicts of Interest statement**

P. Valsasina received speaker honoraria from Biogen Idec.

C. Gobbi and C. Zecca received financial support from Biogen Idec, Celgene, Sanofi, Merck Serono, Novartis, Roche and Teva, not related to the present work.

A. Rovira serves on scientific advisory boards for Novartis, Sanofi-Genzyme, , SyntheticMR, and OLEA Medical, and has received speaker honoraria from Bayer, Sanofi-Genzyme, Merck-Serono, Teva Pharmaceutical Industries Ltd, Novartis, Roche and Biogen Idec.

J. Sastre-Garriga declares grants and personal fees from Genzyme, Almirall, Biogen, Celgene, Merck, Bayer, Biopass, Bial, Novartis, Roche and Teva, outside the submitted work; Dr. Sastre-Garriga is Associate Editor of Multiple Sclerosis Journal and Scientific Director of Revista de Neurologia, outside the submitted work. H. Kearney has received speaking honoraria from Biogen, Roche, and Teva.

M. Yiannakas and P. Eisele have nothing to disclose.

L. Matthews was funded by an MRC fellowship (G0901996).

J. Palace is partly funded by highly specialised services to run a national congenital myasthenia service and a neuromyelitis service. She has received support for scientific meetings and honorariums for advisory work from Merck Serono, Biogen Idec, Novartis, Teva, Chugai Pharma and Bayer Schering, Alexion, Roche, Genzyme, MedImmune, EuroImmun, MedDay, Abide ARGEX, UCB and Viela Bio and grants from Merck Serono, Novartis, Biogen Idec, Teva, Abide, MedImmune, Bayer Schering, Genzyme, Chugai and Alexion. She has received grants from the MS society, Guthrie Jackson Foundation, NIHR, Oxford Health Services Research Committee, EDEN, MRC, GMSI, John Fell and Myaware for research studies.

A. Gallo received speaker and consulting fees from Biogen, Sanofi-Genzyme, Merck Serono and Teva.

A. Biseco received speaker's honoraria and/or compensation for consulting service and/or speaking activities from Biogen, Roche, Merck, Celgene, Coloplast and Genzyme

A Gass has received honoraria for lecturing, travel expenses for attending meetings, and financial support for research from Novartis, Biogen, Merck Serono, Sanofi-Genzyme, Roche.

M. Filippi is Editor-in-Chief of the *Journal of Neurology* and Associate Editor of *Human Brain Mapping*; received compensation for consulting services and/or speaking activities from Almiral, Alexion, Bayer, Biogen, Celgene, Eli Lilly, Genzyme, Merck-Serono, Novartis, Roche, Sanofi, Takeda, and Teva Pharmaceutical Industries; and receives research support from Biogen Idec, Merck-Serono, Novartis, Roche, Teva Pharmaceutical Industries, Italian Ministry of Health,

Fondazione Italiana Sclerosi Multipla, and ARiSLA (Fondazione Italiana di Ricerca per la SLA)., Novartis, Merck-Serono and ExceMED.

M.A. Rocca received speaker honoraria from Bayer, Biogen, Bristol Myers Squibb, Celgene, Genzyme, Merck Serono, Novartis, Roche, and Teva, and receives research support from the MS Society of Canada and Fondazione Italiana Sclerosi Multipla.

## References

1. Gass A, Rocca MA, Agosta F, et al. MRI monitoring of pathological changes in the spinal cord in patients with multiple sclerosis. *Lancet Neurol* 2015;14:443-454.
2. Nijeholt GJ, van Walderveen MA, Castelijns JA, et al. Brain and spinal cord abnormalities in multiple sclerosis. Correlation between MRI parameters, clinical subtypes and symptoms. *Brain* 1998;121 ( Pt 4):687-697.
3. Rocca MA, Horsfield MA, Sala S, et al. A multicenter assessment of cervical cord atrophy among MS clinical phenotypes. *Neurology* 2011;76:2096-2102.
4. Rocca MA, Valsasina P, Meani A, et al. Clinically relevant cranio-caudal patterns of cervical cord atrophy evolution in MS. *Neurology* 2019;93:e1852-e1866.
5. Lukas C, Knol DL, Sombekke MH, et al. Cervical spinal cord volume loss is related to clinical disability progression in multiple sclerosis. *J Neurol Neurosurg Psychiatry* 2015;86:410-418.
6. Moccia M, Prados F, Filippi M, et al. Longitudinal spinal cord atrophy in multiple sclerosis using the generalized boundary shift integral. *Ann Neurol* 2019;86:704-713.
7. Tsagkas C, Magon S, Gaetano L, et al. Preferential spinal cord volume loss in primary progressive multiple sclerosis. *Mult Scler* 2019;25:947-957.
8. Brex PA, Leary SM, O'Riordan JI, et al. Measurement of spinal cord area in clinically isolated syndromes suggestive of multiple sclerosis. *J Neurol Neurosurg Psychiatry* 2001;70:544-547.
9. Rocca MA, Valsasina P, Damjanovic D, et al. Voxel-wise mapping of cervical cord damage in multiple sclerosis patients with different clinical phenotypes. *J Neurol Neurosurg Psychiatry* 2013;84:35-41.
10. Valsasina P, Aboulwafa M, Preziosa P, et al. Cervical Cord T1-weighted Hypointense Lesions at MR Imaging in Multiple Sclerosis: Relationship to Cord Atrophy and Disability. *Radiology* 2018;288:234-244.
11. Khaleeli Z, Ciccarelli O, Manfredonia F, et al. Predicting progression in primary progressive multiple sclerosis: a 10-year multicenter study. *Ann Neurol* 2008;63:790-793.
12. Rocca MA, Sormani MP, Rovaris M, et al. Long-term disability progression in primary progressive multiple sclerosis: a 15-year study. *Brain* 2017;140:2814-2819.
13. Horsfield MA, Sala S, Neema M, et al. Rapid semi-automatic segmentation of the spinal cord from magnetic resonance images: application in multiple sclerosis. *NeuroImage* 2010;50:446-455.
14. Gros C, De Leener B, Badji A, et al. Automatic segmentation of the spinal cord and intramedullary multiple sclerosis lesions with convolutional neural networks. *NeuroImage* 2019;184:901-915.
15. De Leener B, Levy S, Dupont SM, et al. SCT: Spinal Cord Toolbox, an open-source software for processing spinal cord MRI data. *NeuroImage* 2017;145:24-43.
16. Valsasina P, Horsfield MA, Rocca MA, Absinta M, Comi G, Filippi M. Spatial normalization and regional assessment of cord atrophy: voxel-based analysis of cervical cord 3D T1-weighted images. *AJNR American journal of neuroradiology* 2012;33:2195-2200.
17. Eden D, Gros C, Badji A, et al. Spatial distribution of multiple sclerosis lesions in the cervical spinal cord. *Brain* 2019;142:633-646.
18. Kurtzke JF. Rating neurologic impairment in multiple sclerosis: an expanded disability status scale (EDSS). *Neurology* 1983;33:1444-1452.
19. Filippi M, Preziosa P, Copetti M, et al. Gray matter damage predicts the accumulation of disability 13 years later. *Neurology* 2013;81:1759-1767.

20. Filippi M, Preziosa P, Barkhof F, et al. Diagnosis of Progressive Multiple Sclerosis From the Imaging Perspective: A Review. *JAMA Neurol* 2020.
21. Prados F, Moccia M, Johnson A, et al. Generalised boundary shift integral for longitudinal assessment of spinal cord atrophy. *NeuroImage* 2020;209:116489.
22. Ashburner J, Ridgway GR. Symmetric diffeomorphic modeling of longitudinal structural MRI. *Front Neurosci* 2012;6:197.
23. Gilmore CP, Bo L, Owens T, Lowe J, Esiri MM, Evangelou N. Spinal cord gray matter demyelination in multiple sclerosis—a novel pattern of residual plaque morphology. *Brain Pathol* 2006;16:202-208.
24. Bonacchi R, Pagani E, Meani A, et al. Clinical Relevance of Multiparametric MRI Assessment of Cervical Cord Damage in Multiple Sclerosis. *Radiology* 2020;296:605-615.
25. Toosy AT, Kou N, Altmann D, Wheeler-Kingshott CA, Thompson AJ, Ciccarelli O. Voxel-based cervical spinal cord mapping of diffusion abnormalities in MS-related myelitis. *Neurology* 2014;83:1321-1325.
26. Zackowski KM, Smith SA, Reich DS, et al. Sensorimotor dysfunction in multiple sclerosis and column-specific magnetization transfer-imaging abnormalities in the spinal cord. *Brain* 2009;132:1200-1209.
27. Collorone S, Cawley N, Grussu F, et al. Reduced neurite density in the brain and cervical spinal cord in relapsing-remitting multiple sclerosis: A NODDI study. *Mult Scler* 2020;26:1647-1657.
28. Klein JP, Arora A, Neema M, et al. A 3T MR imaging investigation of the topography of whole spinal cord atrophy in multiple sclerosis. *AJNR American journal of neuroradiology* 2011;32:1138-1142.
29. Casserly C, Seyman EE, Alcaide-Leon P, et al. Spinal Cord Atrophy in Multiple Sclerosis: A Systematic Review and Meta-Analysis. *J Neuroimaging* 2018;28:556-586.
30. Hagstrom IT, Schneider R, Bellenberg B, et al. Relevance of early cervical cord volume loss in the disease evolution of clinically isolated syndrome and early multiple sclerosis: a 2-year follow-up study. *J Neurol* 2017;264:1402-1412.
31. Zeydan B, Gu X, Atkinson EJ, et al. Cervical spinal cord atrophy: An early marker of progressive MS onset. *Neurol Neuroimmunol Neuroinflamm* 2018;5:e435.
32. Cortese R, Tur C, Prados F, et al. Ongoing microstructural changes in the cervical cord underpin disability progression in early primary progressive multiple sclerosis. *Mult Scler* 2021;27:28-38.
33. Lin X, Tench CR, Turner B, Blumhardt LD, Constantinescu CS. Spinal cord atrophy and disability in multiple sclerosis over four years: application of a reproducible automated technique in monitoring disease progression in a cohort of the interferon beta-1a (Rebif) treatment trial. *J Neurol Neurosurg Psychiatry* 2003;74:1090-1094.
34. Cawley N, Tur C, Prados F, et al. Spinal cord atrophy as a primary outcome measure in phase II trials of progressive multiple sclerosis. *Mult Scler* 2018;24:932-941.
35. Petrova N, Carassiti D, Altmann DR, Baker D, Schmierer K. Axonal loss in the multiple sclerosis spinal cord revisited. *Brain Pathol* 2018;28:334-348.

**Table 1.** Main demographic, clinical and conventional baseline MRI characteristics of healthy controls (HC) and patients with multiple sclerosis (MS) included in this study. MS patients are first considered as a whole, and then divided according to their clinical phenotype.

	HC	All MS patients	p*	CIS patients	RRMS patients	PMS patients	p*
Males/females	26/28	50/63	0.7 <sup>+</sup>	6/8	33/44	11/11	0.8 <sup>+</sup>
Mean age [years] (IQR)	33.9 (25-40)	42.8 (33-53)	<0.001	31.6 (24-37)	40.9 (32-50) <sup>°</sup>	56.3 (52-62) <sup>§</sup>	<0.001
Median disease duration [years] (IQR)	-	8.2 (2.5-15)	-	0.3 (0.2-0.4)	8.0 (3-15) <sup>°</sup>	10.1 (13-22) <sup>§</sup>	<0.001
Median baseline EDSS score (IQR)	-	2.5 (1.5-4.5)	-	1.0 (0.5-2.0)	2.0 (1.5-3.5) <sup>°</sup>	6.0 (4.5-6.5) <sup>§</sup>	<0.001
Median follow-up EDSS score (IQR)	-	2.5 (1.5-4.5)	-	0.5 (0-2.0)	2.5 (1.5-3.5) <sup>°</sup>	6.5 (5.5-7.0) <sup>§</sup>	<0.001
N (%) of patients receiving DMT at baseline	-	73 (65%)	-	1 (7%)	68 (88%) <sup>°</sup>	4 (18%) <sup>§</sup>	<0.001 <sup>+</sup>
N (%) of patients changing DMT during the follow-up	-	23 (21%)	-	2 (15%)	19 (24%)	2 (9%)	0.3 <sup>+</sup>
Mean number of relapses during the follow-up (range)	-	0.1 (0-2)	-	0.2 (0-2)	0.1 (0-2)	0 (0-0)	0.2 <sup>++</sup>
Median baseline cord lesion # (IQR)	-	2 (0-4)	-	0 (0-1)	2 (0-4)	2.5 (1-5)	0.1 <sup>+</sup>
Median number of new	-	0 (0-0)	-	1 (0-2)	0 (0-0)	0 (0-0.5)	0.1 <sup>++</sup>

cord lesions at follow-up (IQR) -							
Mean baseline brain T2 LV [ml] (SD)	0.01 (0.9)	6.8 (8.1)	<0.001	2.4 (5.5)	6.9 (7.6) °	9.2 (10.3)	<0.001
Mean follow-up brain T2 LV [ml] (SD)	0.02 (0.9)	6.8 (7.6)	<0.001	2.1 (3.9)	6.8 (6.9) °	9.9 (10.1)	<0.001
Mean baseline brain T1 LV [ml] (SD)	-	5.4 (6.9)	-	2.2 (5.1)	5.3 (6.1) °	8.3 (9.8)	0.002
Mean follow-up brain T1 LV [ml] (SD)	-	5.4 (6.8)	-	1.8 (3.4)	4.9 (5.5) °	9.8 (10.1)	0.003
Mean baseline normalized CSA [mm <sup>2</sup> ] (SD)	76.3 (5.6)	73.0 (8.8)	0.4	79.3 (5.5)	74.4 (7.7)	64.0 (8.2) <sup>§</sup>	<0.001
Mean normalized CSA change [%] (SD)	-0.15 (2.0)	-1.61 (2.6)	0.004	0.05 (1.3)	-1.8 (2.6)	-1.9 (2.8)	0.01
Mean baseline NBV [ml] (SD)	1480 (78)	1440 (91)	0.8	1524 (71)	1440 (88)	1382 (68)	0.3
Mean PBVC [%] (SD)	-0.04 (0.4)	-0.32 (0.8)	0.1	0.16 (1.1)	-0.31 (0.7)	-0.79 (0.8)	0.1

<sup>+</sup>Chi-square test; <sup>++</sup>Kruskall-Wallis test; \*age-, sex- (as appropriate) and site-adjusted ANOVA model

*Post hoc* comparisons: °significantly different from CIS; §significantly different from RRMS patients.

Abbreviations: SD=standard deviation; IQR=interquartile range; CIS=clinically isolated syndrome; RRMS=relapsing-remitting multiple sclerosis; PMS=progressive multiple sclerosis; EDSS=Expanded disability status scale; DMT=disease-modifying treatment; LV=lesion volume;

CSA=cord cross-sectional area; NBV=normalized brain volume; PBVC=percentage brain volume change.

**Table 2.** Significant between-group differences of cervical cord atrophy distribution in patients with multiple sclerosis (MS) with different phenotypes (full factorial model adjusted for age, sex, site and total cord volume,  $p < 0.001$ , uncorrected, cluster extent  $k=10$ ). Where clusters survive the family-wise error (FWE) correction for multiple comparisons, they are marked with \* and the family-wise corrected p value is reported.

	Cord level	A/P	R/L	Cluster extent	t value	p
All MS patients vs healthy controls	C1/C2	A	L	156	4.0	<0.001
		A	R	300	3.8	<0.001
		P	L	1410	4.5	0.01*
		P	R	1823	5.3	0.007*
	C3	A	L	-	-	-
		A	R	-	-	-
		P	L	75	3.7	<0.001
		P	R	223	3.6	<0.001
	C4	A	L	-	-	-
		A	R	77	3.3	<0.001
		P	L	-	-	-
		P	R	-	-	-
	C5	A	L	227	4.0	<0.001
		A	R	-	-	-
		P	L	-	-	-
		P	R	174	3.9	0.05*
	C6	A	L	-	-	-
		A	R	-	-	-
		P	L	-	-	-
		P	R	323	3.4	<0.001
CIS vs healthy controls [cord expansion]	C4	A	L	-	-	-
		A	R	-	-	-
		P	L	-	-	-
		P	R	10	3.7	<0.001
RRMS vs CIS	C1/C2	A	L	310	3.8	0.05*
		A	R	86	3.4	<0.001
		P	L	1148	4.2	0.05*
		P	R	282	6.5	0.001*
PMS vs RRMS patients	C1/C2	A	L	90	3.4	<0.001
		A	R	10	3.5	<0.001
		P	L	397	3.8	<0.001
		P	R	100	3.7	<0.001
	C3	A	L	81	4.0	<0.001
		A	R	681	4.2	<0.001
		P	L	143	5.4	0.009*
		P	R	1269	4.8	0.05*

	C4	A	L	162	4.4	<0.001
		A	R	239	3.5	<0.001
		P	L	496	5.2	0.01*
		P	R	779	4.8	0.05*
	C5	A	L	496	3.8	<0.001
		A	R	413	3.9	<0.001
		P	L	401	4.5	0.05*
		P	R	1160	4.4	0.05*
	C6	A	L	517	3.7	<0.001
		A	R	1118	4.5	0.01*
		P	L	517	4.4*	0.01*
		P	R	457	3.8	<0.001
	C7	A	L	485	4.7	0.05*
		A	R	718	3.5	<0.001
		P	L	406	5.0	0.01*
		P	R	727	4.6	0.01*

Abbreviations: CIS=clinically isolated syndrome; RRMS=relapsing-remitting multiple sclerosis;

PMS=progressive multiple sclerosis; R=right, L=left, A=anterior, P=posterior.

**Table 3.** Significant progression of cervical cord atrophy at 1-year visit *vs* baseline in patients with multiple sclerosis (MS), considered as a whole, and in different clinical phenotypes (paired t test adjusted for site, follow-up duration and total cord volume,  $p < 0.001$ , uncorrected, cluster extent  $k=10$ ). Where clusters survive the family-wise error (FWE) correction for multiple comparisons, they are marked with \* and the family-wise corrected p value is reported. Clusters significant at the time-by-group interaction analysis (*vs* HC for all MS patients) are marked with §.

	Cord level	A/P	R/L	Cluster extent	t value	p
All MS patients	C1/C2	A	R	13	3.5	<0.001
		A	L	104	4.1	<0.001
		P	R	556	3.2	<0.001 <sup>§</sup>
		P	L	258	4.5	0.001* <sup>§</sup>
	C3	A	R	-	-	-
		A	L	-	-	-
		P	R	101	4.4	<0.001
		P	L	263	3.9	<0.001
	C4	A	R	-	-	-
		A	L	-	-	-
		P	R	31	3.7	<0.001
		P	L	482	4.1	<0.001
	C5	A	R	-	-	-
		A	L	-	-	-
		P	R	571	4.4	0.01*
		P	L	1177	4.3	0.01*
	C6	A	R	-	-	-
		A	L	-	-	-
		P	R	74	3.6	<0.001
		P	L	-	-	-
RRMS patients	C1/C2	A	R	39	3.6	<0.001
		A	L	103	4.5	0.04*
		P	R	401	4.5	0.001*
		P	L	352	4.7	0.001*
	C3	A	R	10	4.4	0.05*
		A	L	24	3.4	<0.001
		P	R	-	-	-
		P	L	-	-	-
	C4	A	R	37	3.6	<0.001
		A	L	-	-	-
		P	R	385	4.2	0.01*
		P	L	116	3.4	<0.001
	C5	A	R	-	-	-
		A	L	-	-	-
		P	R	336	4.0	0.04*
		P	L	90	3.7	<0.001

	C6	A	R	-	-	-
		A	L	-	-	-
		P	R	38	3.6	<0.001
		P	L	-	-	-
	C7	A	R	-	-	-
		A	L	-	-	-
		P	R	-	-	-
		P	L	22	3.4	<0.001
PMS patients	C1/C2	A	R	30	4.5	<0.001
		A	L	12	4.1	<0.001
		P	R	23	4.3	<0.001
		P	L	-	3.8	<0.001
	C3	A	R	-	-	-
		A	L	-	-	-
		P	R	-	-	-
		P	L	16	3.8	<0.001
	C5	A	R	-	-	-
		A	L	-	-	-
		P	R	-	-	-
		P	L	26	3.8	<0.001

Abbreviations: CIS=clinically isolated syndrome; RRMS=relapsing-remitting multiple sclerosis;

PMS=progressive multiple sclerosis; R=right, L=left, A=anterior, P=posterior.

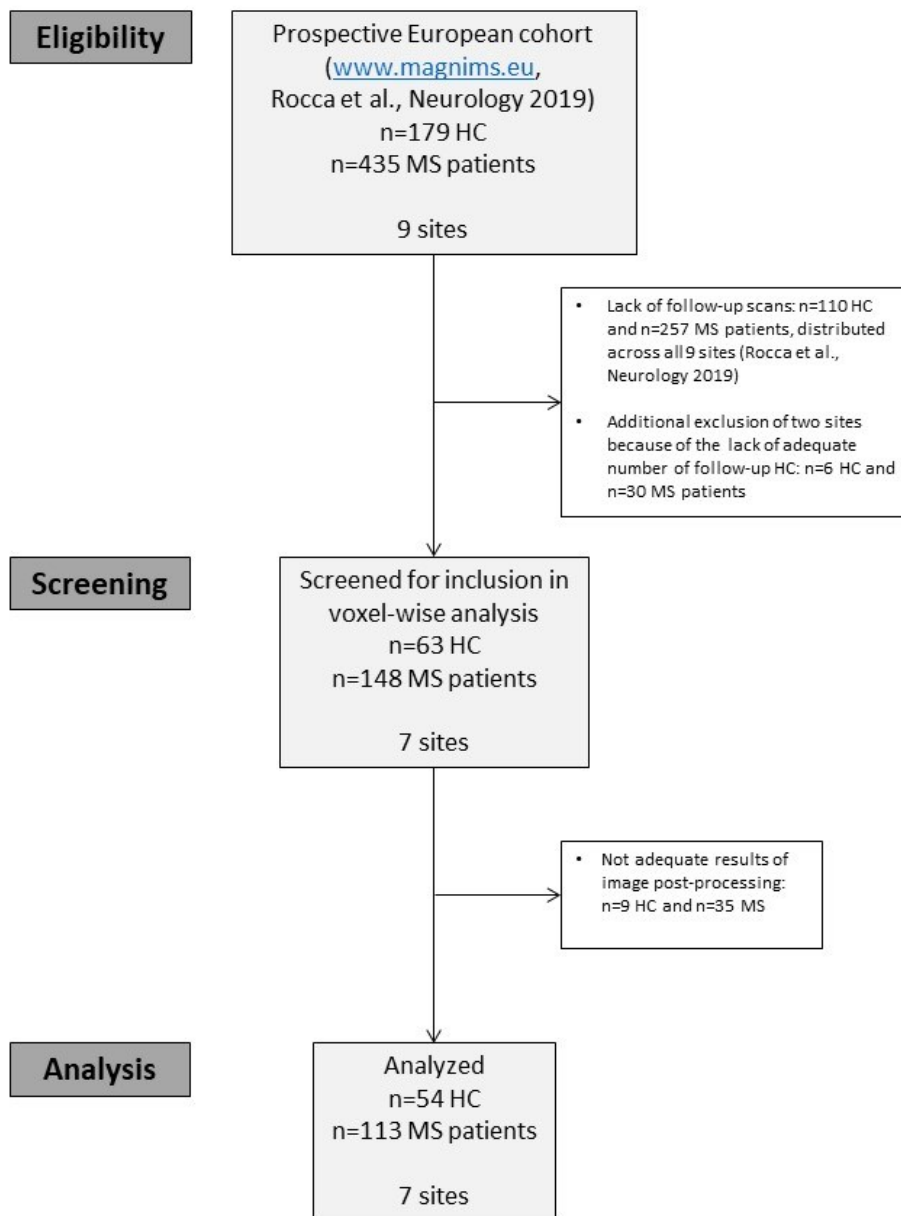


**Figure 1. Study flowchart.** Flowchart showing the main steps of this study, including eligibility assessment, screening and analysis. The number of healthy controls (HC) and patients with multiple sclerosis (MS) undergoing each step, as well as reasons for exclusion, are reported.

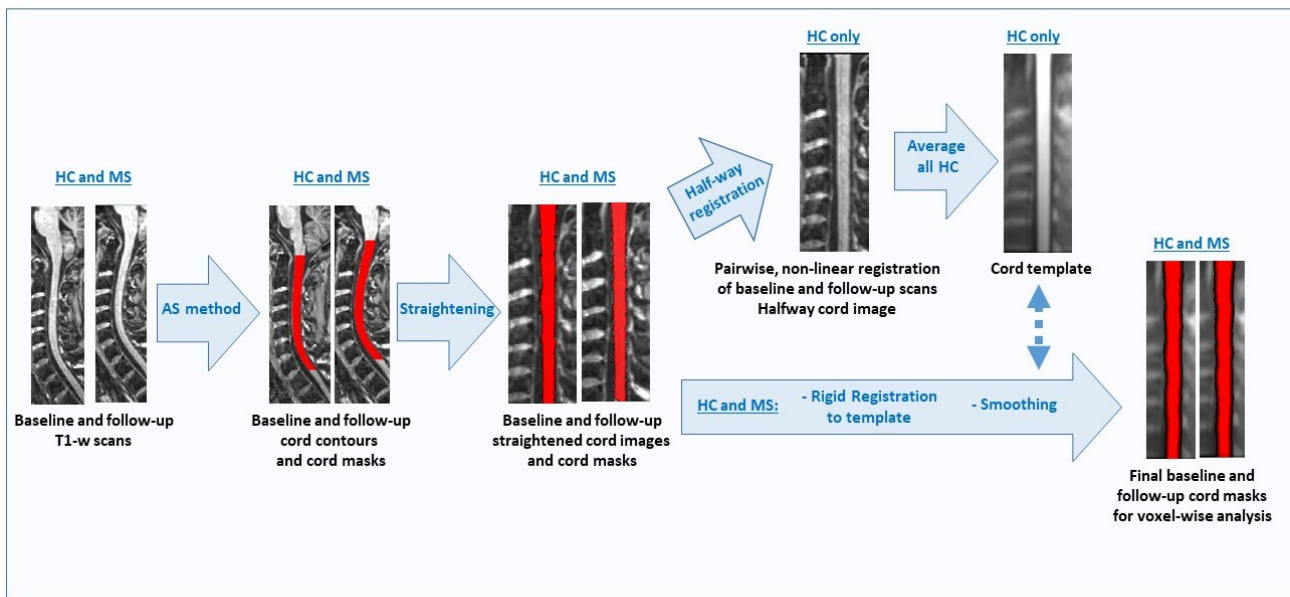


**Figure 2.** Schematic representation of the main processing steps performed on 3D T1-weighted cervical cord scans before voxel-wise analysis. Using the active surface (AS) method (Jim software, version 7.0), cervical cord contours and corresponding cord masks are created on axially reformatted, 1-mm resampled 3D T1-weighted cord images. Then, T1-weighted images are straightened perpendicularly to the estimated cord centre line. Straightened cord images from healthy controls (HC) are co-registered in the half-way space (SPM12, pair-wise registration) and averaged to create a cervical cord template. Baseline and follow-up T1-weighted cord images and corresponding cord masks from all study subjects are then rigidly co-registered to the template (Jim software, version 7.0); finally, cord masks are smoothed ( $1 \times 1 \times 2 \text{ mm}^3$  Gaussian kernel).

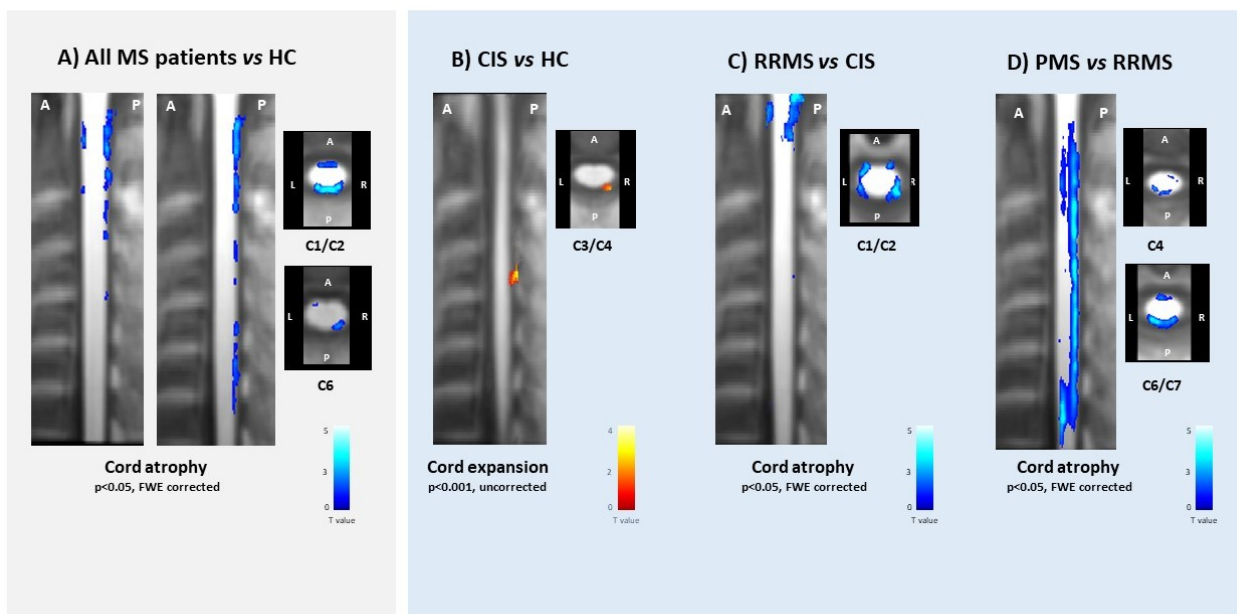


**Figure 3. Regional distribution of cervical cord atrophy at baseline.** Sagittal and axial views of the results of between-group comparisons of regional cervical cord atrophy at baseline. (A) All patients with multiple sclerosis (MS) vs healthy controls (HC); (B) clinically isolated syndrome (CIS) patients vs HC; (C) relapsing-remitting (RR) MS vs CIS patients; and (D) progressive (P) MS vs RRMS patients (color-coded for t-values,  $p < 0.001$  uncorrected, cluster extent  $k = 50$  or  $p < 0.05$ , family-wise error [FWE] corrected, according to significance of each comparison). Abbreviations: A= anterior; P= posterior; L=left; R=right.

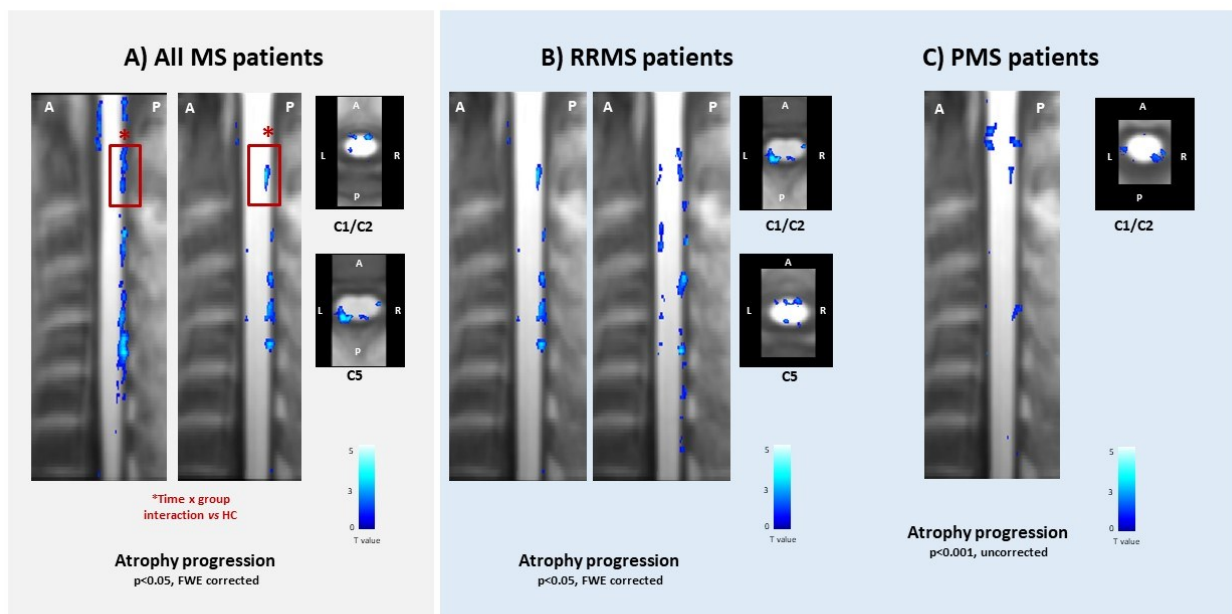


**Figure 4. Regional distribution of cervical cord atrophy progression over time.** Sagittal and axial views of the results of within-group analysis of regional cervical cord progression at 1-year vs baseline. Cord atrophy development was detected in (A) all patients with multiple sclerosis (MS); (B) relapsing-remitting (RR) MS patients; and (C) progressive (P) MS patients (color-coded for t-values,  $p < 0.001$  uncorrected, cluster extent  $k=50$  or  $p < 0.05$ , family-wise error [FWE] corrected, according to significance of each comparison). Red boxes highlight clusters being significant at the time-by-group interaction analysis. Abbreviations: A= anterior; P= posterior; L=left; R=right.

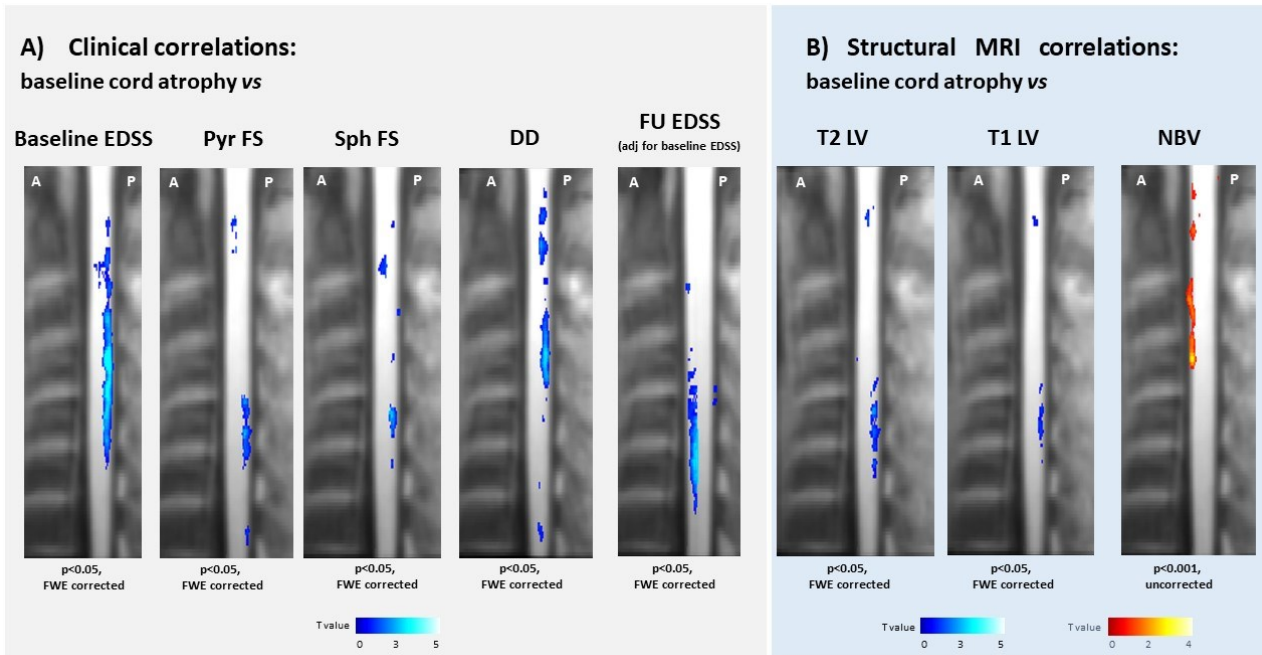


**Figure 5. Regional correlation analysis.** Sagittal views showing significant correlations between baseline regional cord atrophy distribution and clinical/structural MR imaging variables (color-coded for t-values,  $p < 0.001$  uncorrected, cluster extent  $k=50$  or  $p < 0.05$ , family-wise error [FWE] corrected, according to significance of each comparison; red-yellow=positive correlations, blue-lightblue=negative correlations).

(A) Significant correlations between regional cord atrophy and baseline Expanded Disability Status Scale (EDSS) score, pyramidal functional score (FS), sphincteric FS, disease duration (DD) and follow-up (FU) EDSS score (adjusted for baseline EDSS); (B) Significant correlations between regional cord atrophy and brain T2 lesion volume (LV), T1 LV and normalized brain volume (NBV). Abbreviations: A = anterior; P = posterior; L=left; R=right.

**Supplementary Table 1.** Main MRI sequence parameters used at the participating sites.

Sequence	Parameters	Hospital Vall d'Hebron, Barcelona (ES)	University College London, London (UK)	Neurocenter of Southern Switzerland, Lugano (CH)	University of Heidelberg, Mannheim (DE)	IRCCS San Raffaele Scientific Institute, Milan (IT)	University of Campania "Luigi Vanvitelli", Naples (IT)	University of Oxford, Oxford (UK)
Cord 3D T1-weighted scan	TR/TE [ms]	2300/3.2	8/3.7	2300/5.1	1900/2.6	8/"shortest"	7.9/3.2	2300/3.59
	TI [ms]	900	860	1140	1000	"shortest"	450	900
	FA [°]	9	8	8	9	8	20	9
	FOV [mm]	256×240	256×256	256×256	240×240	250×250	250×250	266×200
	Pixel size [mm]	1×1×1	1×1×1	0.98×0.98×1	0.93×0.93×1	1×1×1	1×1×1	1×1×0.9
	# slices /thickness [mm]/ orientation	128/1/Sag	128/1/Sag	104/1/Sag	60/1/Sag	64/1/Sag	60/1/Sag	176/1/Sag
Cord STIR/DE scan	TR/TE [ms]	4000/51	4000/15-80	PD:2000/9 T2:3200/100	3500/108	2463/70	2500/72	4590/67
	TI [ms]	200	-	-	-	200	200	70
	FA [°]	150	90	145	160	120	90	136
	FOV [mm]	280×280	256×256	330×330	300×300	248×130	250×250	250×250
	Pixel size [mm]	0.62×0.62×3.3	1×1×3	0.43×0.43×3.3	0.78×0.78×3.3	0.48×0.48×2.5	0.97×0.97×2.5	0.6×0.6×3
	# slices /thickness [mm]/ orientation	13/3/Sag	12/3/Sag	18/3/Sag	13/3/Sag	14/2.5/Sag	14/2.5/Sag	15/3/Sag
Brain 3D T1-weighted scan	TR/TE [ms]	2300/2.98	6.9/3.14	2300/2.8	1900/2.4	7/3.2	6.9/2.8	2040/4.7
	TI [ms]	900	"shortest"	900	900	900	650	900
	FA [°]	9	8	9	9	8	8	8
	FOV [mm]	256×256	256×256	240×240	240×240	256×240	260×260	192×174

	Pixel size [mm]	1×1×1.2	1×1×1	0.9×0.9×0.9	0.93×0.93×0.9	1×1×1	1.01×1.01×1.2	1×1×1
	# slices /thickness [mm]/ orientation	128/1.2/Sag	180/1/Sag	192/0.9/Sag	192/0.9/Sag	192/1/Sag	166/1.2/Sag	192/1/Tra
Brain FLAIR/ DE scan	TR/TE [ms]	2500/16-91	3500/18-85	2670/18-79	5000/398	2910/16-80	3080/24-120	4670/27-106
	TI [ms]	-	-	-	1800	-	-	-
	FA [°]	123	90	145	120	90	90	150
	FOV [mm]	250×250	240×240	250×250	240×240	240×240	240×240	256×184
	Pixel size [mm]	0.78×0.78×3	1×1×3	0.97×0.97×3.3	0.47×0.47×0.9	0.93×0.93×3	0.47×0.47×3	0.34×0.34×3
	# slices /thickness [mm]/ orientation	46/3/Tra	50/3/Tra	44/3/Tra	192/0.9/Sag	50/3/Tra	44/3/Tra	47/3/Tra

Abbreviations: STIR=short-tau inversion recovery; DE=dual echo; PD=proton density; FLAIR=fluid-attenuated inversion recovery; Tra=transverse; Sag=sagittal; TR=repetition time; TE=echo time; TI=inversion time; FA=flip angle; FOV=field of view.

**Supplementary Table 2.** Significant between-group differences of cervical cord atrophy distribution in patients with multiple sclerosis (MS) with different phenotypes (full factorial model adjusted for age, sex, site and total cord volume,  $p < 0.001$ , uncorrected, cluster extent  $k=10$ ), assessed in patients enrolled in Milan for validation analysis.

	Cord level	A/P	L/R	Cluster extent	t value	p
All MS patients vs healthy controls	C1/C2	A	L	-	-	-
		A	R	-	-	-
		P	L	10	3.4	<0.001
		P	R	47	3.3	<0.001
	C3	A	L	-	-	-
		A	R	10	3.1	<0.001
		P	L	-	-	-
		P	R	-	-	-
	C4	A	L	-	-	-
		A	R	35	3.0	<0.001
		P	L	10	2.9	
		P	R	--	-	-
	C5	A	L	11	3.0	<0.001
		A	R	-	-	-
		P	L	12	2.9	<0.001
		P	R	-	-	-
HC vs RRMS	C1/C2	A	L	-	-	-
		A	R	-	-	-
		P	L	86	3.9	<0.001
		P	R	15	3.1	<0.001
	C3	A	L	-	-	-
		A	R	10	2.8	<0.001
		P	L	-	-	-
		P	R	-	-	-
	C4	A	L	40	2.9	<0.001
		A	R	-	-	-
		P	L	-	-	-
		P	R	12	2.8	<0.001
PMS vs RRMS patients	C1/C2	A	L	-	-	-
		A	R	22	4.3	<0.001
		P	L	10	4.3	<0.001
		P	R	11	4.0	<0.001
	C3	A	L	21	4.1	<0.001
		A	R	-	-	-
		P	L	10	3.9	<0.001
		P	R	14	3.8	<0.001
	C4	A	L	104	4.0	<0.001
		A	R	20	3.8	<0.001
		P	L	-	-	-

		P	R	-	-	-
C5	A	L		37	4.1	<0.001
	A	R		15	3.8	<0.001
	P	L		-	-	-
	P	R		26	4.0	<0.001
C6	A	L		-	-	-
	A	R		-	-	-
	P	L		10	3.9	<0.001
	P	R		14	3.9	<0.001
C7	A	L		67	4.2	<0.001
	A	R		55	4.3	<0.001
	P	L		10	4.0	<0.001
	P	R		60	4.1	<0.001

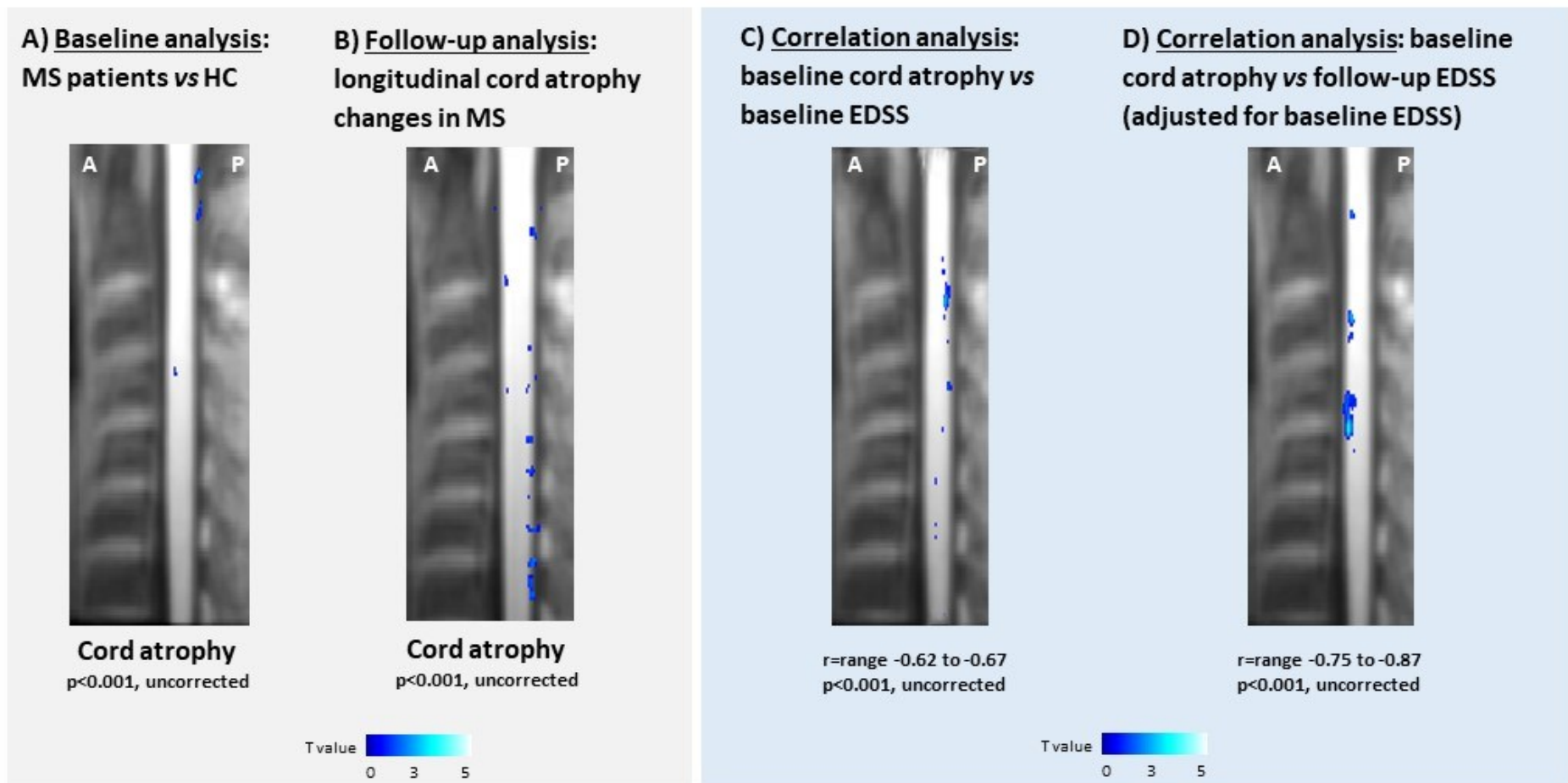
Abbreviations: RRMS=relapsing-remitting multiple sclerosis; PMS=progressive multiple sclerosis;

R=right, L=left, A=anterior, P=posterior.

**Supplementary Table 3.** Significant progression of cervical cord atrophy at 1-year visit vs baseline in patients with multiple sclerosis (MS), considered as a whole, and in different clinical phenotypes (paired t test adjusted for follow-up duration and total cord volume,  $p < 0.001$ , uncorrected, cluster extent  $k=10$ ), assessed in patients enrolled in Milan for validation analysis.

	Cord level	A/P	L/R	Cluster extent	t value	p
All MS patients	C1/C2	A	L	-	-	-
		A	R	-	-	-
		P	L	109	4.3	<0.001
		P	R	50	4.1	<0.001
	C3	A	L	10	4.0	<0.001
		A	R	-	-	-
		P	L	-	-	-
		P	R	12	4.0	<0.001
	C5	A	L	-	-	-
		A	R	10	3.8	<0.001
		P	L	11	3.7	<0.001
		P	R	-	-	-
	C6	A	L	-	-	-
		A	R	-	-	-
		P	L	45	3.7	<0.001
		P	R	86	3.9	<0.001
RRMS patients	C1/C2	A	L	-	-	-
		A	R	10	4.0	<0.001
		P	L	32	4.1	<0.001
		P	R	41	4.2	<0.001
	C6	A	L	-	-	-
		A	R	-	-	-
		P	L	-	-	-
		P	R	26	3.8	<0.001
PMS patients	C1/C2	A	L	16	3.7	<0.001
		A	R	-	-	-
		P	L	20	3.7	<0.001
		P	R	11	3.6	<0.001

Abbreviations: RRMS=relapsing-remitting multiple sclerosis; PMS=progressive multiple sclerosis; R=right, L=left, A=anterior, P=posterior.



**Supplementary Figure 1.** Illustrative examples of voxel-wise analysis of regional cord atrophy performed using data from a single centre (IRCCS San Raffaele Scientific Institute, Milan, Italy) for validation purposes: A) regional distribution of cervical cord atrophy in patients with multiple sclerosis (MS) vs healthy controls (HC) at baseline; B) cord atrophy progression over time in MS patients; C) correlation between baseline cord atrophy and baseline Expanded Disability Status Scale (EDSS) score; and D) correlation between baseline cord atrophy and follow-up (FU) EDSS score (adjusted for baseline EDSS). Results are color-coded for t-values, p<0.001 uncorrected, cluster extent k=10. Abbreviations: A= anterior; P= posterior.